Available online at www.sciencedirect.com
SCIENCE DIRECT®
Polymer 45 (2004) 1971–1979
polymer
www.elsevier.com/locate/polymer

Probing multi-walled nanotube/poly(methyl methacrylate) composites with ionizing radiation

S.R. Tatro[a], L.M. Clayton[a], P.A. O'Rourke Muisener[a], A.M. Rao[b,1], J.P. Harmon[a,*]

[a]Department of Chemistry, University of South Florida, SCA 400, 4202 East Fowler Avenue, Tampa, FL 33620-5250, USA
[b]Department of Physics and Astronomy, Clemson University, 107 Kinard Laboratory, Box 340978, Clemson, SC 29634-0978, USA

Received 11 July 2003; received in revised form 18 December 2003; accepted 9 January 2004

Abstract

Poly(methyl methacrylate) (PMMA) and multi-walled nanotube (MWNT)/PMMA composites were irradiated in air. The constant dose rate was 985 rad/min at a dose of 5.7 Mrad using a Cesium-137 source. The samples were then analyzed by dielectric analysis (DEA), dynamic mechanical analysis (DMA), differential scanning calorimetry (DSC), and Vickers microhardness. The MWNT/PMMA composites were found to show increased radiation hardness with respect to the glass transition temperature and mechanical properties. The dielectric properties were changed more significantly for the composites than for the neat PMMA. In addition, initial aging studies were performed on the irradiated samples after 3 months via DMA. The results indicate that multi-walled nanotubes may enhance radiation hardness of mechanical properties in PMMA.

Keywords: Multi-walled nanotubes; DEA; Ionizing radiation

1. Introduction

This study focuses on the radiation effects on the mechanical and dielectric properties of multi-walled nanotube/poly(methyl methacrylate) (MWNT/PMMA) composites. The radiation effects of PMMA has been extensively studied [1–14]. When exposed to γ and ultraviolet radiation in air and under vacuum, main chain scission is the dominant occurrence [2,5,14]. The degradation of the polymer is indicated by a decrease in the glass transition temperature [5,14] and the evolution of products including monomer, hydrogen gas, carbon dioxide, carbon monoxide, methane, and propane [2,14].

Studies continue to focus on developing new methods for increasing the radiation resistance of polymeric materials since radiation exposure is a concern in many polymer applications. The smaller the extent of molecular changes due to irradiation, the more radiation resistant the material. When aromatic groups are incorporated into the polymer, either within the structure or as an additive, they can increase its radiation resistance. The aromatic groups absorb the excitation energy; and, because of the efficiency with which the excited states return to the ground states, a lower bond cleavage yield is noted [15,16]. This, in turn, causes a decrease in the formation of free radicals, which are responsible for scission, cross-linking and other degradation reactions.

Researchers have tried to limit radiolysis products in polymers via the use of additives [15,16]. Two of the most prevalent types of additives are excited-state energy scavengers and electron scavengers. Aromatics are the most common type of energy scavengers, and are able to act as energy traps. Excitation energy, which has been absorbed by the polymer matrix, is then able to migrate throughout the polymer. The aromatic additives absorb the excitation and release it in the form of light or heat energy, thus reducing the number of free radicals formed.

We were the first group to suggest the use of single-walled carbon nanotubes as radiation hardening agents [17,18]. Tang and Xu have also demonstrated that nanotubes exhibit a strong photostablilization in poly(phenyl acetylene)-wrapped carbon nanotube structures [19]. These conjugated structures were first observed in 1991 in multi-wall form [20–22]. Multi-walled nanotubes consist of concentric tubes, which are one atomic monolayer each. In

* Corresponding author. Tel.: +1-813-974-3397; fax: +1-813-974-1733.
E-mail addresses: harmon@chuma1.cas.usf.edu (J.P. Harmon), arao@clemson.edu (A.M. Rao).
[1] Tel.: +1-864-656-6758; fax: +1-864-656-0805.

0032-3861/$ - see front matter © 2004 Elsevier Ltd. All rights reserved.
doi:10.1016/j.polymer.2004.01.012

1993, the discovery of single-walled nanotubes [21–24] increased interest in the field, but because of their short supply, the majority of studies continued to focus on more easily synthesized multi-walled nanotubes. Carbon nanotubes exhibit armchair, chiral, and zigzag geometries. Each tube is usually capped by half of a fullerene [21,22]. Carbon nanotubes are classified as a one-dimensional carbon system because of their high aspect ratio [25]. Past studies have indicated that nanotubes behave as stiff elastic rods with low density [26–29]. Recent efforts identified numerically the unrealized technical potential for designing composites with superior mechanical, thermal, transport, optical and electronic properties [30]. Previously, nanotube composites have been developed using many different polymer matrices, including PMMA [31–37]. Methods for fabrication of the composites include incorporating pure or functionalized nanotubes via sonication, either with the monomer or in dimethyl formamide with the previously synthesized polymer, and melt processing [17,18,31,38–43]. It is extremely important to optimize composite processing techniques. The carbon nantoube and polymer properties, as well as, the quality of the dispersion and the interaction between the filler and polymer affect the performance of the composite [42,43]. Experimental studies have shown that PMMA nanotube composites demonstrate an increase in electrical conductivity, melt viscosity, and elastic modulus as the concentration increases [29,36,38].

In previous studies, our laboratory investigated the effects of γ radiation on poly(methyl methacrylate)/single-walled nanotube composites [17,18]. These composites where studied by differential scanning calorimetry (DSC), Vickers microhardness measurements, dielectric analysis (DEA), and dynamic mechanical analysis (DMA). The PMMA/SWNT composites after exposure to γ radiation, exhibited very little change in the glass transition temperature, the Vickers hardness number, and modulus, indicating increased radiation resistance. The DEA data for both the neat PMMA and the composite, however, showed an increase in the loss factor and permittivity after irradiation. This study examines the γ radiation effects in MWNT/PMMA composites to determine if a similar increase in radiation hardness is obtained with more readily available multi-walled nanotubes. In addition, the authors note the importance of understanding radiation–oxidation events that occur when polymers are exposed to air during or after irradiation. Many experiments document the effect of post irradiation aging on chemical and physical properties [14,44–46]. Herein we include initial results from an ongoing study involving post irradiation aging of the irradiated MWNT/PMMA composites. Specifically, DMA was performed on samples aged three months in air.

2. Experimental materials

The methyl methacrylate (MMA) monomer was purchased from Aldrich (Milwaukee, WI), and the 2,2′-azobis(2,4-dimethylpentane nitrile) (VAZO 52) initiator was purchased from DuPont (Wilmington, DE). The solvents used were reagent grade dichloromethane, reagent grade methanol, and Certified A.C.S. grade *N*,*N*-dimethyl formamide (DMF), purchased from Fisher Scientific (Pittsburgh, PA). The monomethyl ether hydroquinone (MEHQ) inhibitor was removed from the MMA using a MEHQ inhibitor remover column available from Aldrich (Milwaukee, WI). All other materials were used without further purification.

2.1. Polymer synthesis

Poly(methyl methacrylate) (PMMA) was synthesized via addition polymerization. 0.2 wt% of the initiator, 2,2′-azobis[2,4-dimethylvaleronitrile] was added to the deinhibited methyl methacrylate monomer and polymerized in bulk at 60 °C for 18 h. The resulting polymer was then dissolved in methylene chloride precipitated in methanol to remove any impurities, and dried under vacuum at 110 °C for two days.

2.2. Multi-walled nanotube (MWNT) synthesis

The multiwalled carbon nanotubes (MWNTs) were produced by a thermal CVD process [47]. Approximately 0.345 g of ferrocene was dissolved in 3 g of *o*-xylene to obtain a feed solution with ~0.75 at% Fe/99.25 at% C ratio. The feed solution was fed continuously into a two-stage tubular quartz reactor (operated at near atmospheric pressure) using a syringe pump at a rate of 1 ml/h. The liquid feed after passing through the first-stage (maintained at 200 °C) of the reactor gets volatilized and swept into the second-stage (maintained at 750 °C) of the reactor by a flow of argon (675 sccm) and hydrogen (75 sccm) [47]. Carbon deposits were formed on the walls of the quartz reactor tube and on bare quartz substrate (microscopic slides) that were placed within quartz tube to act as additional sites for nanotube growth. The deposits were extracted and characterized using scanning electron microscopy (SEM) (Figs. 1 and 2). A dense mat of aligned MWNTs were revealed in the SEM images, and electron diffraction patterns obtained on individual MWNT showed the presence of 002 reflections confirming a high degree of structural order.

2.3. Multiwall nanotube/poly(methyl methacrylate) composites

The MWNTs were sonicated in DMF for 2 h with a Branson Sonifier 450. The DMF containing the dispersed MWNTs was then combined with a 10% (w/v) PMMA/DMF solution. This mixture was sonicated an additional 2 h. The PMMA was then precipitated out of solution using methanol. The resulting 1 wt% MWNT/PMMA composite was dried under vacuum at 110 °C for two days and

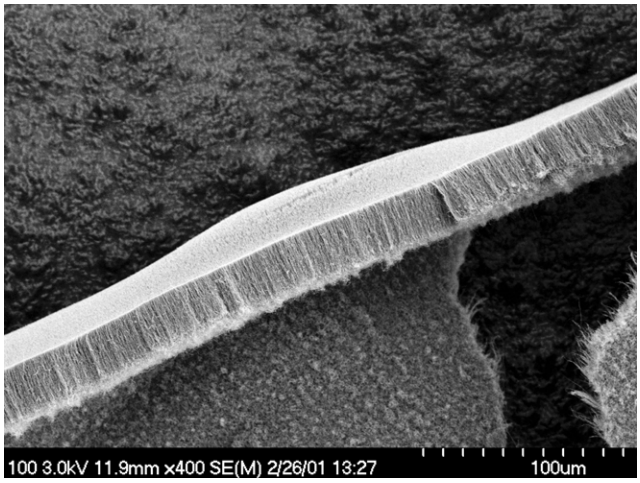

Fig. 1. SEM image of the edge of a MWNT array grown using xylene–ferrocene mixtures at ~700 °C in Argon flow [47].

then at 140 °C for an additional two days. The remaining neat PMMA was also processed using this technique

The 1 wt% MWNT/PMMA composite was mixed with neat PMMA using a C.W. Brabender Plasticorder® with a banbury mixer attachment to create 0.10, 0.26, and 0.50 wt% MWNT/PMMA composites. Composites were characterized via SEM to capture the dispersion of the MWNT in the polymer matrix (Fig. 3).

2.4. Molding

Samples were compression molded at 135 °C and 3000 lbs of pressure for 15 min in a Carver Press.

2.5. Irradiation

All samples (excluding the controls) were γ-irradiated in air at room temperature via a ^{137}Cs source. The dose rate was constant at 985 rad/min for a total dose of 5.7 Mrad. Harshaw TLD-400 (CaF_2/Mn) thermoluminescent ribbon dosimeters (TLDs) were used along with a Harshaw 5500 TLD reader to determine dose rates. The dosimeter dimensions were 0.32 cm × 0.32 cm × 0.09 cm thickness with a use limit up to 1 MeV. Dosimetry testing provided absorbed dose rate values (rads (Si)/min) used to prepare an isodose contour map. The resultant map identified sample positioning for the dose rate of 985 rad/min.

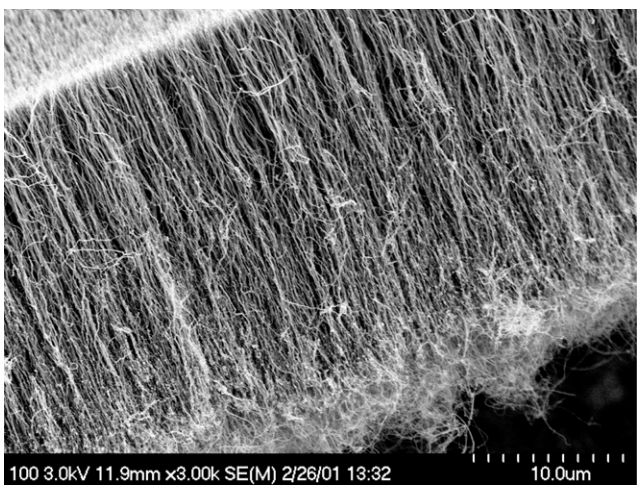

Fig. 2. SEM of the edge of the MWNT array: expanded view [47].

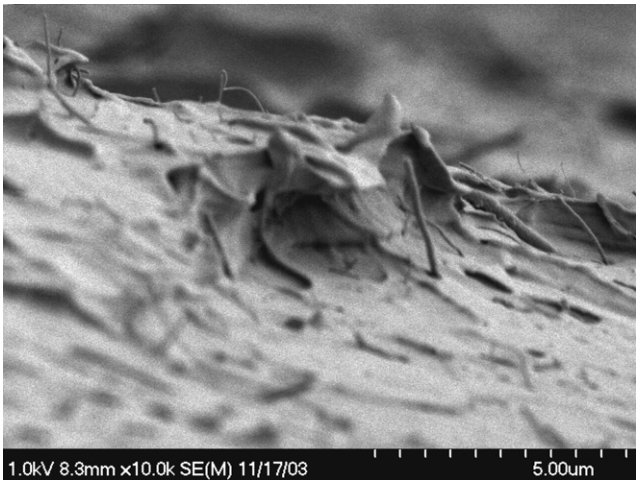

Fig. 3. SEM of MWNT/PMMA composite.

2.6. Dielectric analysis (DEA)

Dielectric data were collected using a TA Instruments 2970 DEA. The analysis was conducted under nitrogen purge from a temperature of 200 to −150 °C in increments of −5 °C. Parallel plate sensors were used. A maximum force of 250 N was applied to the samples that reached a range of thickness from 0.3 to 1.4 mm. The permittivity (e'), loss factor (e'') and tan δ were recorded at frequencies ranging from 1 to 1.0×10^6 Hz.

2.7. Differential scanning calorimetry (DSC)

A TA Instruments 2920 DSC was used to determine the glass transition temperatures of the PMMA and the MWNT/PMMA composites. Samples from 7 to 10 mg were scanned under a nitrogen purge at a ramp rate of 10 °C/min. Glass transition temperatures were determined on the second scan to assure identical thermal histories.

2.8. Microhardness

A Leica VMHT MOT with a Vickers indenter was used to determine the Vickers hardness number (HV). Four indents were made on each sample using a load of 500 g and a dwell time of 20 s. The Vickers hardness number is based on the average diagonal length of an imprint made from the indentor. Both the horizontal and vertical diagonal length was measured for each indent. The values reported are an average of these eight measurements.

2.9. Dynamic mechanical analysis (DMA)

DMA data were collected with a TA Instruments 2980 dynamic mechanical analyzer in tension mode. 1–100 Hz was the frequency range examined with an amplitude of 5 μm. Measurements were taken from −150 to 150 °C in 5 °C increments. The average sample size was 18 × 5 × 2 mm. Tests were repeated after three months of aging at room temperature in air.

3. Results and discussion

3.1. Dielectric analysis

When PMMA is analyzed by DEA, two separate transitions can be seen. The first transition, α, corresponds to main chain motion, and the second transition, β, corresponds to rotation of the side group. For PMMA, at high temperatures and frequencies, the two transitions merge to give an $\alpha\beta$ relaxation, which is attributed to cooperative side group rotation and main chain motion [12,14,48–51]. Over a wide range of temperatures (−150 to 200 °C) and frequencies (1–10^6 Hz), the permittivity (ε'), the loss factor (ε''), and tan δ were recorded. Over the frequency range in which α and β did not overlap, the inverse of the temperature at maximum peak height was plotted against the natural log of the frequency to determine activation energies. Data for the β relaxation followed the expected Arrhenius behavior. Activation energies for the β process are listed in Table 1. All of the samples exhibit similar activation energies (18–19 kcal/mol) indicating that neither the addition of the carbon nanotubes nor irradiation affected the ease with which the side groups rotate. The Williams, Landel, and Ferry (WLF) equation [52,53], which is often applicable to the α transition of amorphous polymers could not be applied to our system as a result of extensive merging of the the α and β relaxations.

Fig. 4 is a plot of ε'' vs. temperature for each of the samples. The transition seen is the β transition at 1 Hz. For the non-irradiated samples there is a decrease in peak height as the concentration of MWNT's is increased. By viewing this in conjunction with the permittivity, the energy required to bring the dipoles to maximum alignment must be less as a result of limited rotation. Once the samples have been irradiated, the trend is reversed. This is also illustrated by the increase in percent change at maximum peak height (Table 2). As the concentration of nanotubes is increased the percent change also increases.

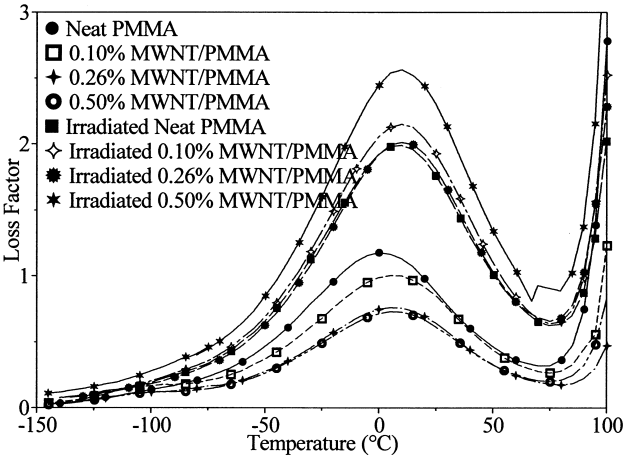

Fig. 4. DEA data: loss factor (ε'') vs. temperature for irradiated and non-irradiated PMMA and MWNT/PMMA nanocomposites at 1 Hz.

The ε' vs. temperature plot (Fig. 5), for the samples before irradiation, shows a decrease in permittivity as the concentration of MWNT's is increased. The authors attribute this to the alignment of the dipoles being limited as a result of hindrance caused by the presence of the MWNT's.

Tan δ vs. temperature is shown in Fig. 6. According to McCrum [52], PMMA has two additional secondary transitions. One which corresponds to the rotation of the methyl group attached to the ester side chain and one which corresponds to the methyl group attached directly to the backbone. Neither of these rotations result in a directional change in net dipole moments and are not normally observed via dielectric spectroscopy, but are seen in dynamic mechanical experiments. The peak assigned to the α methyl group rotation is observed at temperatures from −20 to −150 °C [52]. The rotation of the $-CH_3$ group about the O–C bond in the ester group occurs at extremely low temperatures, below −250 °C [52]. Before irradiation, in each of the nanotube composites, there is an additional relaxation seen in the dielectric data at around −100 °C. This transition is absent in the neat polymer samples. The authors interpret this to be a direct indication that interactions between the nanotubes and polymer groups are responsible for the γ relaxation, making it visible via DEA. This relaxation has also been seen in PMMA/SWNT

Table 1
DEA data for irradiated and non-irradiated PMMA: activation energies for the β transition (kcal/mol)

Sample	Control	5.7 Mrad
Neat	18	19
0.1% MWNT/PMMA	19	19
0.26% MWNT/PMMA	19	19
0.5% MWNT/PMMA	18	18

Table 2
DEA data for irradiated and non-irradaited PMMA: loss factor (ε'') at maximum peak height for β transition at 1 Hz

Sample	Control	5.7 Mrad	Percent change
Neat PMMA	1.18	1.99	68.6
0.10% MWNT/PMMA	1.00	2.15	115
0.26% MWNT/PMMA	0.760	2.01	165
0.50% MWNT/PMMA	0.730	2.56	250

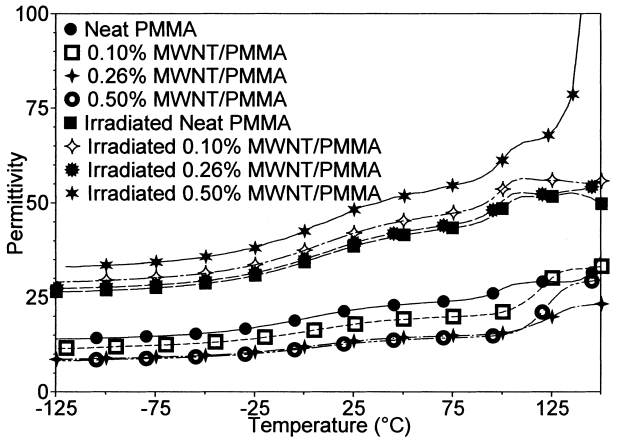

Fig. 5. DEA data: permittivity (ε') vs. temperature for irradiated and non-irradiated PMMA and MWNT/PMMA nanocomposites at 1 Hz.

composite studies conducted by the authors [54]. Additionally, it has been stated in literature that carbon nanotubes can be used to identify or detect polymer relaxations [55]. Activation energies could not be obtained for this additional transition due to significant merging with the β transition at higher frequencies. This transition is no longer visible after irradiation, indicating possible structural changes within the nanotubes themselves or changes at the polymer-nanotube interface. Morphological changes in carbon nanotubes due to γ radiation have been evidenced previously via scanning electron microscopy [17,18].

Further analysis of the dielectric data was performed using the Havriliak–Negami equation (1) [56,57] This equation provides an empirical equation with which to represent the data.

$$\frac{\varepsilon^*(\omega) - \varepsilon_U}{\varepsilon_R - \varepsilon_U} = [1 + (i\omega\tau_0)^{1-\alpha}]^{-\beta} \quad (1)$$

Where ε_U is the unrelaxed state that would be seen at infinitely high frequencies, ε_R is the relaxed state that would be seen as the frequency approaches zero, τ_0 is the relaxation time, α is the parameter correlating to broadening of the curve, and β is the parameter correlating to the skew of the curve [49].

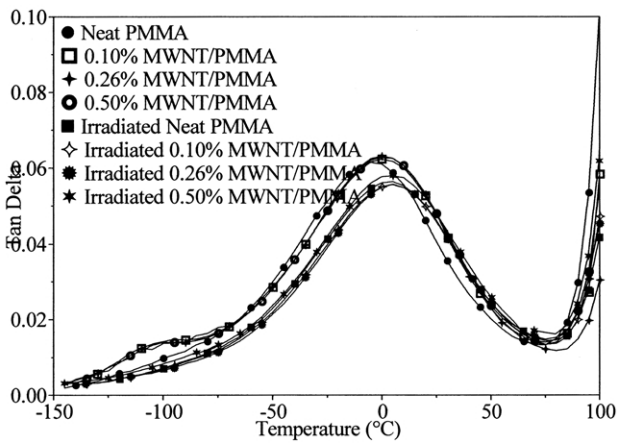

Fig. 6. DEA data: tan δ vs. temperature for irradiated and non-irradiated PMMA and MWNT/PMMA nanocomposites at 1 Hz.

By plotting ε' vs. ε', the parameters ε_U and ε_R can be determined from the two intercepts on the ε' axis. The first intercept represents the unrelaxed state that would be seen at infinitely high frequencies (ε_U), while the second intercept represents the completely relaxed state seen at very low frequencies (ε_R). The relaxation strength, $\Delta\varepsilon$, is the difference between these two values and is defined in the following equation:

$$\Delta\varepsilon = \varepsilon_R - \varepsilon_U \quad (2)$$

For this study, ε' was plotted against ε'' at 45 °C, a temperature corresponding to the β relaxation. To determine the dielectric strengths and the α and β parameters a fitting program was developed. Table 3 displays the dielectric data determined from the Havriliak–Negami plots. In the non-irradiated samples, there is a slight decrease in $\Delta\varepsilon$ as the nanotube concentration is increased. After irradiation, the dielectric strengths of the samples are similar, with the exception of the 0.50% MWNT/PMMA sample, which is significantly higher. There is an obvious trend for the percent change of the dielectric strength before and after irradiation for each of the different nanotube concentrations (Table 4). The percent change for the neat sample is only 68.03% and increases dramatically for each concentration until reaching a percent change of 273.3% for the 0.50% MWNT/PMMA sample. This behavior indicates gamma radiation results in a larger number of dipoles as the concentration of multi-walled nanotubes is increased, which may be due to radiation induced charge build up on the nanotube surfaces.

3.2. Differential scanning calorimetry

DSC was used to determine the glass transition temperatures (T_g) before and after irradiation. The T_g for the neat PMMA before irradiation was determined to be 125 °C. As the concentration of multi-wall carbon nanotubes increases there is a very slight increase in the glass transition temperature indicating the possibility that main chain motion is hindered by the carbon nanotubes. After

Table 3
DEA Havriliak–Negami data for irradiated and non-irradiated MWNT/PMMA nanocomposites: 45 °C

Sample	$10^2 \times \tau$	α	β	ε_U	ε_R	$\Delta\varepsilon$]
Neat control	5.0	0.4970	0.4380	13.140	23.480	10.340
0.10% Control	7.9	0.4981	0.4440	11.087	19.584	8.497
0.26% Control	8.9	0.5020	0.4280	8.140	14.650	6.510
0.50% Control	7.9	0.5010	0.4560	7.970	14.090	6.120
Neat irradiated	11.4	0.4990	0.4200	25.040	42.414	17.374
0.10% Irradiated	11.0	0.4940	0.4280	27.773	46.138	18.365
0.26% Irradiated	12.1	0.4952	0.4208	25.945	43.216	17.271
0.50% Irradiated	12.7	0.4930	0.3950	30.330	53.173	22.843

Table 4
DEA Havriliak–Negami data for irradiated and non-irradiated MWNT/PMMA nanocomposites: percent change at 45 °C

Sample	Percent change
Neat PMMA	68.03
0.10% MWNT/PMMA	113.3
0.26% MWNT/PMMA	165.1
0.50% MWNT/PMMA	273.3

irradiation, there is a decrease in all of the glass transition temperatures; however, the decrease in the neat, 0.1% MWNT/PMMA, and 0.26% MWNT/PMMA samples were significantly higher than the decrease for the 0.5% MWNT/PMMA sample (Table 5). It has been previously reported that PMMA undergoes scission when exposed to gamma radiation in air and results in a decrease in the molecular weight. The decrease in the molecular weight illustrated by the decrease in glass transition temperature for the first three samples is consistent with that referenced in the literature for PMMA undergoing scission [58,59]. The smaller decrease in T_g in the 0.5% MWNT/PMMA sample is explained by increased radiation hardness as a result of the higher concentration of nanotubes. This increase in radiation hardness between the 0.26 and 0.50% samples may be a result of reaching the percolation threshold. The lack of change in T_g in the 0.50% MWNT/PMMA indicates a decrease in scission. This decrease in scission is expected in the presence of additives containing aromatic groups, which can act as radiation sinks [15,16].

3.3. Microhardness

The Vickers hardness number was determined for each of the samples. As the concentration of multi-wall nanotubes in the composite is increased from 0.00% (neat PMMA) to 0.50%, there is an increase in the Vickers hardness number from 20.9 to 24.6, respectively (Table 6). Once the samples have been irradiated the neat PMMA and 0.10% MWNT/PMMA, exhibited a decrease in the Vickers hardness number. The 0.26% MWNT/PMMA, gave a very slight decrease in the Vickers hardness number while the 0.5% MWNT/PMMA showed a significant increase in the hardness. The increase in the Vickers hardness number for the 0.50% MWNT/PMMA irradiated sample supports the hypothesis that radiation hardness increases with greater

Table 5
DSC glass transition temperature (T_g) data for irradiated and non-irradiated PMMA nanocomposites (°C)

Sample	Control	5.7 Mrad
Neat	125	111
0.1%	125	110
0.26%	127	112
0.5%	127	124

Table 6
Vickers hardness number

Sample	Control	5.7 Mrad	Percent change
Neat	20.9 ± 0.8	19.0 ± 0.1	−9.09
0.10% MWNT/PMMA	22.0 ± 0.6	20.1 ± 0.6	−8.64
0.26% MWNT/PMMA	23.1 ± 0.2	22.7 ± 0.6	−1.73
0.50% MWNT/PMMA	24.6 ± 0.9	26.6 ± 0.6	+8.13

nanotube concentration and suggests the possibility of limited cross-linking at higher nanotube concentrations. It has been reported that in some instances, irradiation can cause carbon nanotubes to be 'soldered' forming mechanical junctions [60–63].

3.4. Dynamic mechanical analysis

DMA can be used to examine the elastic and viscous properties of a polymeric material. The storage modulus (E') represents the elastic properties of the polymer and demonstrates the stiffness, and the loss modulus (E'') represents the viscous properties of the polymer. The storage modulus at 10 Hz is shown in Fig. 7 for temperatures from 100 to 150 °C. All of the non-irradiated samples show similar behavior; however, after irradiation, E' decreases for all samples. The decrease is larger for both the neat PMMA and the 0.1% MWNT/PMMA composite than for the 0.26 and 0.50% MWNT/PMMA composites. E' changes very little after irradiation for the 0.26 and 0.50% MWNT/PMMA composite. The samples were also aged for three months and then tested via DMA. As shown in Fig. 8, the storage modulus of irradiated MWNT/PMMA composites did not change with aging. However, the storage modulus decreased for the neat PMMA sample aged for three months, indicating increased degradation. All of the irradiated samples bubbled, after heating above the glass transition temperature. For the samples tested immediately following radiation exposure, the amount and size of the

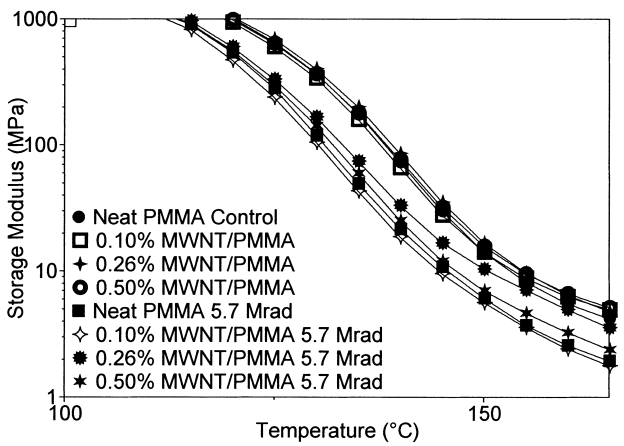

Fig. 7. DMA data: storage modulus (E') vs. temperature for irradiated and non-irradiated PMMA and MWNT/PMMA nanocomposites at 10 Hz (expanded view): samples tested immediately following radiation exposure.

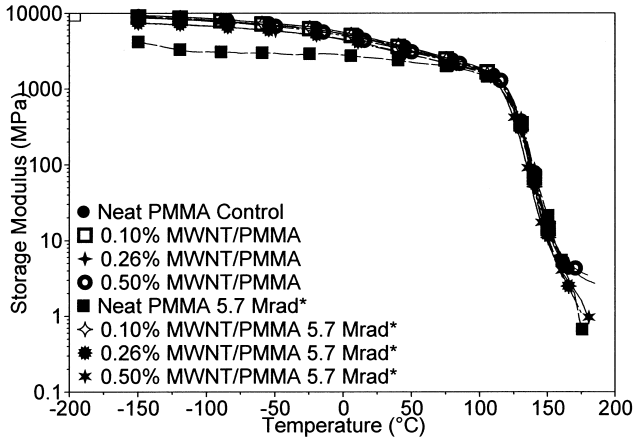

Fig. 8. DMA data: storage modulus (E') vs. temperature for irradiated and non-irradiated PMMA and MWNT/PMMA nanocomposites at 10 Hz: samples tested three months following radiation exposure.

bubbles were relatively consistent from sample to sample. The neat PMMA sample tested at three months showed a significant increase in bubbling when compared to the neat PMMA sample tested immediately following exposure. However, for the composites, there was no apparent increase in bubbling after aging.

The loss modulus data (E'') before and after aging are shown in Figs. 9 and 10. In the E'' plots, two transitions are apparent: α transition corresponding to main chain molecular motion, and the β transition corresponding to the rotation of the ester side group [46]. The inverse of the temperature at maximum peak height was plotted vs. the natural log of the frequency to determine the activation energies (Table 7). A linear relationship was found indicating the β relaxation exhibited Arrhenius behavior. The activation energies for most of the samples remain relatively constant except for the aged neat PMMA whose activation energy increased to 25 kcal/mol. Similar to the storage modulus data, the most significant changes in the E'' data after irradiation occurs in the neat PMMA and the 0.1% MWNT/PMMA samples.

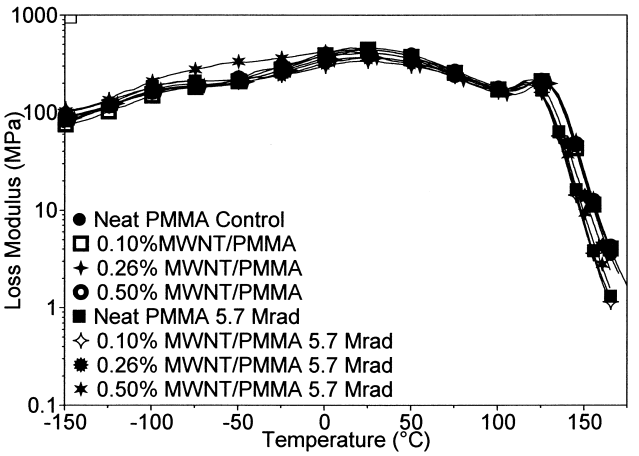

Fig. 9. DMA data: loss modulus (E'') vs. temperature for irradiated and non-irradiated PMMA and MWNT/PMMA nanocomposites at 10 Hz: samples tested immediately following radiation exposure.

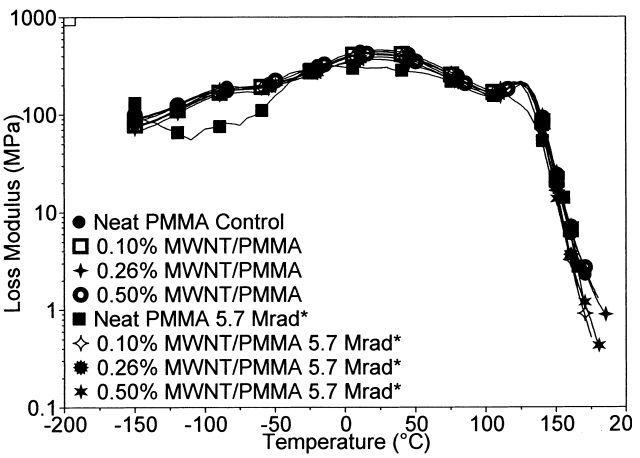

Fig. 10. DMA data: loss modulus (E'') vs. temperature for irradiated and non-irradiated PMMA and MWNT/PMMA nanocomposites at 10 Hz: samples tested three months following radiation exposure.

These initial aging studies indicate that the irradiated composites appear to exhibit stable mechanical properties. However, extended aging studies are needed to document the persistence of this effect.

4. Conclusions

This initial study reveals that dielectric properties change dramatically with radiation. Furthermore, the extent of change increases as the nanotube concentration increases. The conductive nature of carbon nanotubes renders these structures labile to dramatic changes in dielectric properties due to possible radiation-induced changes within the nanotubes and changes in charge distribution at the interface between the polymer and nanotubes. Mechanical properties of the composites are less labile to radiation-induced events. The conjugated bonds of the carbon nanotubes may, to some extent, absorb radiation energy and return efficiently to the ground state, thus, limiting damage to the PMMA molecules. There is an increase in the radiation resistance for the 0.50% MWNT/PMMA composite, indicating the possibility of having reached the percolation threshold. By reaching a concentration above the percolation limit, the carbon nanotubes may have increased the ability to absorb and transfer radiant energy. This study indicates that the radiation resistance of PMMA may be increased through the addition of very minute amounts of multi-walled carbon nanotube. However, further aging studies are required to verify the persistence of this phenomenon. Future studies will be extended to include Raman data and further structural analysis of the polymer-nanotube interfaces.

Acknowledgements

We would like to thank All Children's Hospital in St. Petersburg, Florida for the use of their irradiator and

Table 7
DMA data for irradiated and non-irradiated PMMA: activation energies for the β transition (kcal/mol)

Sample	Control	5.7 Mrad tested immediately	5.7 Mrad tested at three months
Neat	19	18	25
0.1% MWNT/PMMA	19	16	17
0.26% MWNT/PMMA	17	17	18
0.5% MWNT/PMMA	18	17	20

Honeywell, Inc. in Clearwater, Florida for performing dosimeter experiments.

References

[1] Kudoh H, Sasuga T, Seguchi T, Katsumura Y. Polymer 1996;37:4663.
[2] Reich L, Stivala S. Elements of polymer degradation. New York: McGraw-Hill; 1971.
[3] Shrempel F, Witthuhn W. Nucl Instrum Methods Phys Res Sect B 1997;132:430.
[4] Ichikawa T, Oyama K, Kondoh T, Yoshida H. J Polym Sci: Part A: Polym Chem 1994;32:2487.
[5] Goyanes SN, Benites GM, González JJ, Rubiolo GH, Marzocca AJ. Polym Test 1997;16:7.
[6] Okudaira KK, Morikawa E, Hasegawa S, Sprunger PT, Saile V, Seki K, Harada Y, Ueno N. J Electron Spectrosc 1998;88–89:913.
[7] Goyanes SN, Benites GM, Rubiolo GH, Marzocca J. J Phys III 1996; 6:587.
[8] Sayyah SM, Sabbah AI, Ayaub MMH, Barsoum BN, Elwy E. Polym Degrad Stab 1997;58:1.
[9] El-Salmawi K, Abu Zeid MM, El-Naggar AM, Mamdouh M. J Appl Polym Sci 1999;72:509.
[10] Gaynor J, Schueneman G, Schuman P, Harmon JP. J Appl Polym Sci 1993;50:1645.
[11] Harmon JP, Gaynor JF, Taylor AG. Radiat Phys Chem 1993;41:153.
[12] Bertolucci PRH, Harmon JP. Polym Engng Sci 1998;38:699.
[13] Harmon JP, Gaynor JF. J Polym Sci: Part B: Polym Phys 1993;31:235.
[14] Tatro SR, Baker GR, Bisht K, Harmon JP. Polymer 2003;44:167–76.
[15] Clough RL, Gillen KT, Dole M. In: Clegg DW, Collyer AA, editors. Irradiation effects on polymers. New York: Elsevier; 1991. p. 116.
[16] Clough RL, Gillen KT. Radiation resistance of polymers and composites. New York: Elsevier; 1991.
[17] Harmon JP, Muisener PAO, Clayton L, D'Angelo J, Sikder AK, Kumar A, Meyyappan M, Cassell A. Mater Res Soc Symp ProceedingsFall 2002;697:P9.7.1–P9.7.11.
[18] O'Rourke Muisener PA, Clayton L, D'Angelo J, Harmon JP. J Mater Res 2002;17:2507.
[19] Tang BZ, Xu H. Macromolecules 1999;32:2569–76.
[20] Iijima S. Nature 1991;354:56.
[21] Dresselhaus MS, Dresselhaus G, Eklund PC, Saito R. Optical and electronic properties of fullerenes and fullerene-based materials. New York: Marcel Dekker; 2000.
[22] Shinar J, Vardeny ZV, Kafafi ZH. Optical and electronic properties of fullerenes and fullerene-based matericals. New York: Marcel Dekker; 2000.
[23] Iijima S, Ichihashi T. Nature 1993;363:603.
[24] Bethune DS, Kiang CH, de Vries MS, Gorman G, Savoy R, Vazquez J, Beyers R. Nature 1993;363:605.
[25] Dresselhaus MS, Dresselhaus G, Eklund PC. Science of fullerenes and carbon nanotubes. San Diego: Academic Press; 1995.
[26] Salvetat J, Kulik AJ, Bonard J, Andres G, Briggs D, Stöckli T, Méténierks, Bonnamy S, Béguin F, Burnham NA, Forró L. Adv Mater 1999;11:161.
[27] Treacy MMJ, Ebbesen TW, Gibson JM. Nature 1996;381:678.
[28] Wong EW, Sheehan PE, Lieber CM. Science 1997;277:1971.
[29] Falvo MR, Clary GJ, Taylor II RM, Chi V, Brooks Jr FP, Washburn S, Superfine R. Nature 1997;389:582.
[30] Gusev A. Macromolecules 2001;34:3081–93.
[31] Haggenmueller R, Gommans HH, Rinzer AG, Fischer JE, Winey KI. Chem Phys Lett 2000;330:219.
[32] Jia Z, Wang Z, Xu C, Liang J, Wei B, Wu D, Zhu S. Mater Sci Engng 1999;271:395.
[33] Shaffer MS, Windle AH. Adv Mater 1999;11:937.
[34] Jin L, Bower C, Zhou O. Appl Phys Lett 1998;73:1197.
[35] Andrews R, Jacques D, Rao AM, Rantell T, Derbyshire F, Chen Y, Haddon RC. Appl Phys Lett 1999;75:1329.
[36] Sandler J, Shaffter MSP, Prasse T, Bauhofer W, Schulte K, Windle AH. Polymer 1999;40:5967.
[37] Stéphan C, Nguyen TP, Lamy de la Chapelle M, Lefrant S, Vaccarini L, Bernier P. Synth Mater 2000;108:139.
[38] Qian D, Dickey EC, Andrews R, Rantell T. Appl Phys Lett 2000;76: 2868.
[39] Star A, Stoddart JF. Macromolecules 2002;35:7516–20.
[40] Tang BZ, Xu H. Macromolecules 1999;32:2569–76.
[41] Hill DE, Lin Y, Rao AM, Allard LF, Sun YP. Macromolecules 2002; 35:9466–71.
[42] Barrau S, Dermon P, Peigney A, Laurent C, Lacabanne C. Macromolecules 2003;36:5187–94.
[43] Hill DE, Lin Y, Rao AM, Allard LF, Sun Y-P. Macromolecules 2002; 35:9466–71.
[44] Alam TM, Celina M, Assink RA, Clough RL, Gillen KT. Radiat Phys Chem 2001;60:121–7.
[45] Gillen KT, Clough RL. Polym Mater Sci Engng 1985;52:586–91.
[46] Clough R. Radiation resistant polymers. In: Kroschwitz J, editor. Encyclopedia of polymer science and engineering, vol. 13. New York: Wiley; 1988. p. 667–708.
[47] Andrews R, Jacques D, Rao AM, Derbyshire F, Qian D, Fan X, Dickey EC, Chen J. Chem Phys Lett 1999;303:467.
[48] Emeran SK, Liu Y, Newkome GR, Harmon P. J Polym Sci: Part B: Polym Phys 2001;39:1381.
[49] Calves MC, Harmon JP. Miscibility investigation of fluorocarbon copolymer and methacrylate copolymer blends. Washington DC: American Chemical Society; 2001.
[50] Harmon JP, Noren GK. Optical polymers: fibers and waveguides. Washington DC: American Chemical Society; 2001.
[51] Gao H, Harmon JP. Thermochem Acta 1996;284:85.
[52] McCrum NG, Read BE, Williams G. Anelastic and dielectric effects in polymeric solids. New York: Dover; 1967.
[53] Emran SK. Doctoral dissertation: viscoelastic properties of dendrimers, dendrimer blends, and dendrimer gels. Tampa: University of South Florida; 2000.
[54] Clayton LM, Sikder AK, Kumar A, Cinke M, Meyyappan M, Gerasimov TG, Harmon JP. Adv Funct Mater 2004; in press.
[55] Zhao Q, Wood J, Wagner HD. J Polym Sci: Part B: Polym Phys 2001; 39:1492.

[56] Runt JP, Fitzgerald JJ. Dielectric spectroscopy of polymeric materials. Washington DC: American Chemical Society; 1997.
[57] Havriliak S, Negami S. J Polym Sci Symp Ser 1966;14:99.
[58] Hill DJT, Milne KA, O'Donnell JH, Pomery PJ. ACS Symp Ser Irradiation Polym 1996;620:130–8.
[59] Dong L, Hill DJT, O'Donnell JH, Pomery PJ, Hatada K. J Appl Polym Sci 1996;59:589–97.
[60] Banhart F. Nano Lett 2001;1:329.
[61] Krasheninnikov AV, Nordlund K, Sirvio M, Salonen E, Keinonen K. Phys Rev 2001;63:24505.
[62] McCarthy B, Coleman JN, Curran SA, Dalton AB, Davey AP, Konya Z, Fonseca A, Nagy JB, Blau WJ. J Mater Sci Lett 2000; 19:2239.
[63] Hwang GL, Hwang KC. Nano Lett 2001;8:435.